Science of the Total Environment 949 (2024) 174960

Contents lists available at ScienceDirect

Science of the Total Environment

journal homepage: www.elsevier.com/locate/scitotenv

Differential contribution of microbial and plant-derived organic matter to soil organic carbon sequestration over two decades of natural revegetation and cropping

Hongling Qin [a,1], Yi Liu [a,1], Chunlan Chen [a], Anlei Chen [a], Yuting Liang [b], Carolyn R. Cornell [c], Xue Guo [d], Edith Bai [e], Haijun Hou [a], Dou Wang [a], Leyan Zhang [a], Jingyuan Wang [a], Dongliang Yao [a], Xiaomeng Wei [f], Jizhong Zhou [g], Zhiliang Tan [a], Baoli Zhu [a,*]

[a] Key Laboratory of Agro-ecological Processes in Subtropical Region, Institute of Subtropical Agriculture, Chinese Academy of Sciences, Changsha 410125, China
[b] Key Laboratory of Soil and Sustainable Agriculture, Institute of Soil Science, Chinese Academy of Sciences, Nanjing 210008, China
[c] Department of Civil and Environmental Engineering, Rice University, Houston, TX, USA
[d] Key Laboratory of Urban and Regional Ecology, Research Center for Eco-Environmental Sciences, Chinese Academy of Sciences, Beijing 100085, China
[e] Key Laboratory of Geographical Processes and Ecological Security of Changbai Mountains, Ministry of Education, Northeast Normal University, Changchun 130024, China
[f] College of Resources and Environment, Northwest Agriculture and Forestry University, Yangling 712100, China
[g] Institute for Environmental Genomics and Department of Microbiology and Plant Biology, University of Oklahoma, Norman, OK, USA

HIGHLIGHTS

- SOC substantially increased over two decades of natural revegetation compared to cropland.
- Greater contribution of plant-derived C to SOC in natural revegetation than in cropland
- Vegetation and microorganisms synergistically contributed to long-term SOC sequestration.

GRAPHICAL ABSTRACT

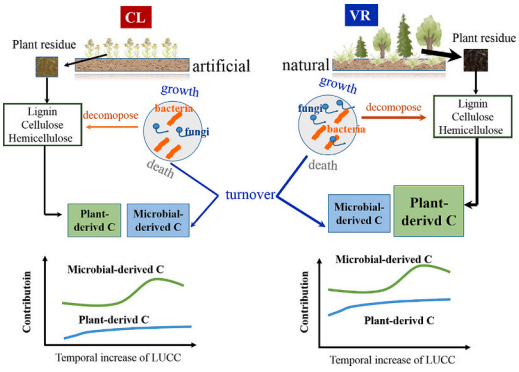

ARTICLE INFO

Editor: Jay Gan

Keywords:
Land use change
Temporal dynamics
Recalcitrant organic carbon

ABSTRACT

Both natural revegetation and cropping have great impact on long-term soil carbon (C) sequestration, yet the differences in their underlying mechanisms remain unclear. In this study, we investigated trends in soil organic C (SOC) accumulation during natural revegetation (VR) and cropping processes over 24 years, and explored the contributions of microbial necromass and plant-derived C to SOC formation and their primary controls. Over the course of 24 years of land use/cover change (LUCC) from 1995, SOC content exhibited a more substantial

* Corresponding author.
E-mail address: baoli.zhu@isa.ac.cn (B. Zhu).
[1] These authors contributed equally.

https://doi.org/10.1016/j.scitotenv.2024.174960
Received 12 May 2024; Received in revised form 16 July 2024; Accepted 20 July 2024
Available online 30 July 2024

Microbial necromass
Biotic and abiotic factors

increase in VR (0.31 g kg^{-1} a^{-1}) than in cropland (0.14 g kg^{-1} a^{-1}) during Stage II (>10 y after LUCC), and recalcitrant organic carbon explained more of the SOC variation than easily oxidizable carbon. The higher SOC content in VR was attributed to a greater contribution of plant-derived C (14–28 %) than that in cropland (3–11 %) to SOC and a consistently lower ratio of cinnamyl (C)- to vanillyl (V)-type phenols in VR across all the assessed years. Although there were higher proportion of microbial necromass of SOC (41–84 %) in cropland than in VR, the differences were not significant. The dominant bacterial phylum of Chloroflexi and soil nitrogen content were the primary biotic and abiotic factors regulating microbial-derived and plant-derived C in both cropland and VR. However, soil phosphorus content was the main factor in cropland, while climatic factors such as mean annual precipitation were more important in VR. These results provided evidence that long-term natural revegetation enhanced SOC sequestration by greater contribution of plant-derived C to SOC formation compared to cropping. These findings underscore the synergistic contribution of vegetation and microorganisms to long-term SOC sequestration, offering insights into the different mechanisms of carbon formation during VR and cropping processes, and providing support for optimizing land management to achieve global carbon neutrality goals.

1. Introduction

Land use/cover change (LUCC) has a direct and significant impact on soil carbon storage in terrestrial ecosystems (IPCC, 2019). Globally, carbon emissions resulting from LUCC amounted to 0.9 ± 0.7 Gt C globally in 2020 (Friedlingstein, 2021). Among various land use types, soil organic C (SOC) is highest in forests and lowest in farmland (Wasige et al., 2014). Revegetation of degraded ecosystems on a global scale serves as a vital strategy for carbon sequestration, contributing to carbon neutrality by offsetting anthropogenic carbon emissions (Bastin et al., 2019; Wang and Huang, 2020). Natural revegetation (VR) can alter both the input and decomposition rates of organic matter, thereby influencing soil C content (Rennert et al., 2018; Ghani et al., 2023). Nevertheless, our current understanding of the mechanisms driving dynamic changes in SOC following LUCC and the processes of organic matter input and decomposition that directly influence SOC accumulation remain limited.

Soil organic matter (SOM) is a complex mixture of plant- and microbial-derived polymers and their degradation products (Angst et al., 2021). Identifying the source of SOC as plant- or microbial-derived components helps to understand its formation pathways and the mechanisms underlying SOC stability (Huang et al., 2023). The "Humification theory" suggests that plant residues, particularly lignin and other complex molecules, are primary contributors to SOC (Schmidt et al., 2011). However, emerging theories, such as the microbial carbon pump propose that microorganisms play a central role in regulating the sequestration of stable SOC by breaking down plant residues into smaller fragments through *ex vivo* modification and assimilating them *via in vivo* turnover (Liang et al., 2019). Contrary to this, recent studies have shown that plant residues may preferentially bind to minerals, occupying a larger proportion of aggregates and mineral components compared to microbial residues (Angst et al., 2021; Chang et al., 2021). Currently, the contributions of plant- or microbial-derived C to long-term SOC formation remains debated.

The spatial and temporal distribution of microbial-derived and plant-derived C (PC) exhibit strong heterogeneity, influenced by environmental conditions (Kan et al., 2022; Camenzind et al., 2023). On a larger spatial scale, climate conditions such as annual average temperature, annual precipitation, *etc.* mainly drive changes in plant- and microbial-derived C (Chen et al., 2020). The soil properties, such as moisture content, pH value, bulk density, soil C/N, and soil aeration conditions, also have a significant impact on the formation and stability of plant- and microbial-derived C (Buckeridge et al., 2020). In addition, changes in microbial abundance and community structure can significantly affect soil SOC cycling and storage (Ma et al., 2020a, 2020b). After land change, soil properties will inevitably change, which will indirectly change plant- and microbial-derived C. However, exploring the potential regulatory mechanisms of factors such as soil physicochemical properties and microbial traits at the spatiotemporal scale is crucial.

Long-term experiments are pivotal in advancing ecological theory by elucidating the evolutionary mechanisms of ecological processes and providing foundational parameters (Ladau and Eloefadrosh, 2019; Dai et al., 2020). At the Taoyuan Agroecosystem Research Station in Hunan Province, China, an ongoing land use experiment since 1995 investigates transformations in degraded *Camellia* forests through VR and cropland (CL) practices, and soil samples have been collected every five years, creating an archive of soil series and allowing assessment of the temporal dynamics of microbial communities over several decades. With over two decades of constant managements under distinct land uses, this site offers an ideal opportunity to investigate SOC stability and formation. In this study, we hypothesize that the contributions of plant- and microbe-derived organic matter to soil organic carbon sequestration differ over two decades of natural revegetation and cropping and are influenced by environmental conditions. The objectives of this study were to: (1) determine trends in SOC, microbial-derived C and PC pools over time post-LUCC and (2) evaluate the contribution of microbial-derived C and PC to SOC and the controlling factors in CL and VR. Overall, our findings underscore the significance of preserving microbial-mediated C turnover processes to maintain SOC after LUCC, a crucial strategy in mitigating future climate change.

2. Materials and methods

2.1. Research sites and sample collection

This study was conducted at a long-term sloped land use experimental site (Fig. S1a) at the Taoyuan Agroecosystem Research Station (111°26′ E, 28°55′ N; altitude 92.2–125.3 m) of the Institute of Subtropical Agriculture, Chinese Academy of Sciences (Changsha City, Hunan Province). The region is characterized by a subtropical humid monsoon climate, with an annual average air temperature of 16.5 °C, precipitation of 1448 mm, sunshine for 15 h and 13 min, and a frost-free period of 283 days (Fig. S1b–c). The experiment was established in 1995, sloped land of *Camellia* forest was ploughed and divided into seven land use plots (with area of 62 m × 20 m), and each type of land use consisted three replicates (20 m × 20 m) at upper, middle, and lower slope positions. Here the natural revegetation and cropping lands were investigated, ten soil cores along a "S" shaped line were collected (0–20 cm) at each replicate site and mixed thoroughly. Soil samples were collected in 2001, 2005, 2010, 2015, and 2019. In total, 30 soil samples were collected (2 land use types × 3 replicate sites × 5 time points). Natural revegetation was developed from grass, shrubs, and young trees mixed under natural vegetation from 1995 to 2019. As comparison, CL was planted with a two-year rotation of corn–rape–potato–turnip and maintained under conventional management as described by Qin et al. (2013).

2.2. Analysis of soil properties

All soil samples were air-dried and sieved through a 2 mm mesh size

for long-term preservation. Soil organic C content was determined using dichromate oxidation (Lu, 2000). Easily oxidizable C (EOC) was quantified by oxidation with 333 mM $KMnO_4$, and recalcitrant organic C (ROC) was calculated by subtracting EOC from SOC (Blair et al., 1995). As described by Lu (2000), the pH value of the soil was measured using a pH meter with a soil:water ratio of 1:2. Available N (AN) content was determined using the alkaline-hydrolyzed diffusion method. Available P (AP) was extracted with ammonium fluoride and hydrochloric acid solution, and its content was determined using molybdenum-antimony colorimetry. Available K (AK) content was determined using the flame photometric method. Total N (TN) concentration was measured using an AA3 continuous flow analyzer after digestion with H_2SO_4 and extraction with 1 M KCl. Total P (TP) content was determined using the molybdophosphate method that digested the soil with a mixture of $HClO_4$ and H_2SO_4 before measuring with an AA3 continuous flow analyzer. Total K (TK) content was determined using a melt flame photometer after melting by sodium hydroxide. Cation exchange capacity (CEC) was determined using the ammonium acetate exchange method. Additionally, soil Zn, Cu, Fe, Pb, Cr, and Ni contents were determined by inductively coupled plasma-mass spectrometry, and the soil was digested with a mixture of HCl-HNO_3-HF-$HClO_4$.

2.3. Amino sugar analysis for microbial necromass estimation

The content of amino sugars was measured as a surrogate for MNC. Soil amino sugars were extracted as previously described by Zhang and Amelung (1996). Briefly, the amino sugars in the soil samples were hydrolyzed, purified, and derived using gas chromatography, as previously described by Ni et al. (2021). Bacterial and fungal MNC (BNC and FNC, respectively) contents were measured from the concentrations of MurN and GluN, respectively, based on empirical conversion factors. Fungal MNC content was determined by subtracting bacterial glucosamine content from total glucosamine content, assuming that MurN and GluN occur at a 1:2 M ratio in bacterial cells.

$$FNC = (GluN/179.17 - 2 \times MurN/251.23) \times 179.2 \times 9 \quad (1)$$

where, 179.2 is the molecular weight of GluN and 9 is the conversion value of fungal GluN to FNC (Appuhn and Joergensen, 2006).

$$BNC = MurN \times 45 \quad (2)$$

where, 45 is the conversion factor for the transformation of MurN to BNC (Appuhn and Joergensen, 2006). Total MNC was estimated as the sum of FNC and BNC values.

2.4. Lignin phenol analysis for plant-derived C

Lignin phenols were extracted using alkaline CuO oxidation to release lignin monomers, followed by gas chromatography (GC-7890B, Agilent Technologies, Santa Clara, CA, USA) according to the method developed by Hedges and Ertel (1982). Briefly, 0.1–0.2 g soil was mixed with 400 mg CuO, 100 mg ammonium iron (II) sulfate hexahydrate ($Fe(NH_4)_2(SO_4)_2{\cdot}6H_2O$), and 15 mL of 2 M NaOH solution in a Teflon vessel. All vessels were flushed with N_2 in the headspace for 20 min heated at 150 °C for 2 h and left 25 °C overnight. The oxidation products were dissolved by 50 μL *N*,*O*-bis-(trimethylsilyl) trifluoroacetamide, and 10 μL pyridine at 70 °C for 3 h to yield trimethylsilyl derivatives. Process details and modes can be found in a study by Chen et al. (2021). Lignin phenols were quantified as the sum of vanillyl (V)-, syringyl (*S*)-, and cinnamyl (C)-type phenols. The C/V ratio indicates the degree of microbial alteration and oxidation of lignin (Li et al., 2020). The PC in total SOC (P) is estimated by the following equation:

$$P(\%) = (V/33.3\% + S/90\% + C)/22.5\% \times SOC \times 100\%$$

Two thirds of the V phenols in lignin structures are not released by CuO oxidation, whereas S phenols are released with 90 % efficiency. The release efficiency of C phenols is assumed to be 100 % (Hautala et al., 1997). The average lignin content in plant residues was considered to be 22 % (Jung et al., 2015).

2.5. DNA extraction and high-throughput sequencing

Microbial DNA was extracted from 0.5 g air-drying soil using a FastDNA Spin Kit for Soil (MP Biomedicals, Santa Ana, CA, USA, Edwards et al., 2024). DNA quality and concentrations were measured using a NanoDrop NA-1000 spectrophotometer (Nanodrop Technologies, Wilmington, DE, USA). The extractions were repeated three times, and the contents were pooled and stored at −80 °C until analysis. The bacterial *16S rRNA* gene was amplified by polymerase chain reaction (PCR) using primers 338F (5′-ACTCCTACGGGAGGCAGCA3′) and 806R (5′-GGACTACHVGGGTWTCTAAT-3′) (Langille et al., 2013). The fungal *ITS* gene was amplified using primers ITS1F (5′-CTTGGTCATTTAGAGGAAGTAA-3′) and ITS2 (5′-GCTGCGTTCTTCATCGATGC-3′) (Nilsson et al., 2019) for high-throughput sequencing. High-throughput sequencing was performed at Majorbio Bio-pharm Technology Co., Ltd. (Shanghai, China) using the Illumina PE300 platform. Sequence analysis was performed using Mothur software (version v.1.30.2; https://mothur.org). The sequences were denoised, checked for chimeras, and clustered based on 97 % identity.

2.6. Data processing and statistical analysis

One-way analysis of variance (ANOVA) was performed using the SPSS statistical software (SPSS20 Inc., Chicago, IL, USA) with a least-significant difference (LSD) *post hoc* test to assess the effect of land use and succession time on the content of SOC, fractions of ROC and EOC, amino sugars and MNC, lignin phenols, and PC. The following analyses were performed in R software (version 4.2.0; http://www.r-project.org/). Random forest using the "randomForest" package was performed to identify the predictive environmental variables for PC and microbial-derived C. The environmental variables selected included soil geochemical properties (AN, AP, AK, TN, TP, TK, pH, and CEC), climate conditions (mean annual temperature (MAT) and mean annual precipitation (MAP)). The accuracy importance measure was computed for each tree and averaged over the forest (5000 trees). Percentage increases in the mean squared error (MSE) of variables were used to estimate the importance of these predictors, with higher MSE% values implying more important predictors. Pearson's correlation coefficients were used for determining the relationships between environmental variables and PC and microbial-derived C.

3. Results

3.1. Temporal dynamics of soil organic C after land use change

After 24 years of LUCC starting in 1995, the development of SOC was divided into two stages: Stage I being earlier, slow changes (<10 y after LUCC), and Stage II being later, more rapid increases (>10 y after LUCC). The increase in SOC content was found to be greater in VR (0.31 g kg^{-1} a^{-1}) than that in CL (0.14 g kg^{-1} a^{-1}) at Stage II (Fig. 1a). At Stage I, minimal differences in SOC were observed; however, there was a significant ($P < 0.05$) decrease in EOC and an increase in ROC contents in CL and VR. At Stage II, the increase in ROC content played a major role in the overall increase in SOC content in VR, where the rate of increase in ROC was greater at 0.23 g kg^{-1} a^{-1} compared to EOC at 0.09 g kg^{-1} a^{-1}, while the rates of increase in EOC and ROC were similar in CL (Fig. 1b–c).

Recalcitrant organic C represented the dominant portion of SOC at Stage II, which was higher than that at Stage I and accounted for, on average, 65.67 % and 62.31 % of SOC in VR and CL, respectively (Fig. S2a). Variance Partitioning Analysis (VPA) for Stage II further indicated that ROC in VR and CL explained more of the variation in SOC

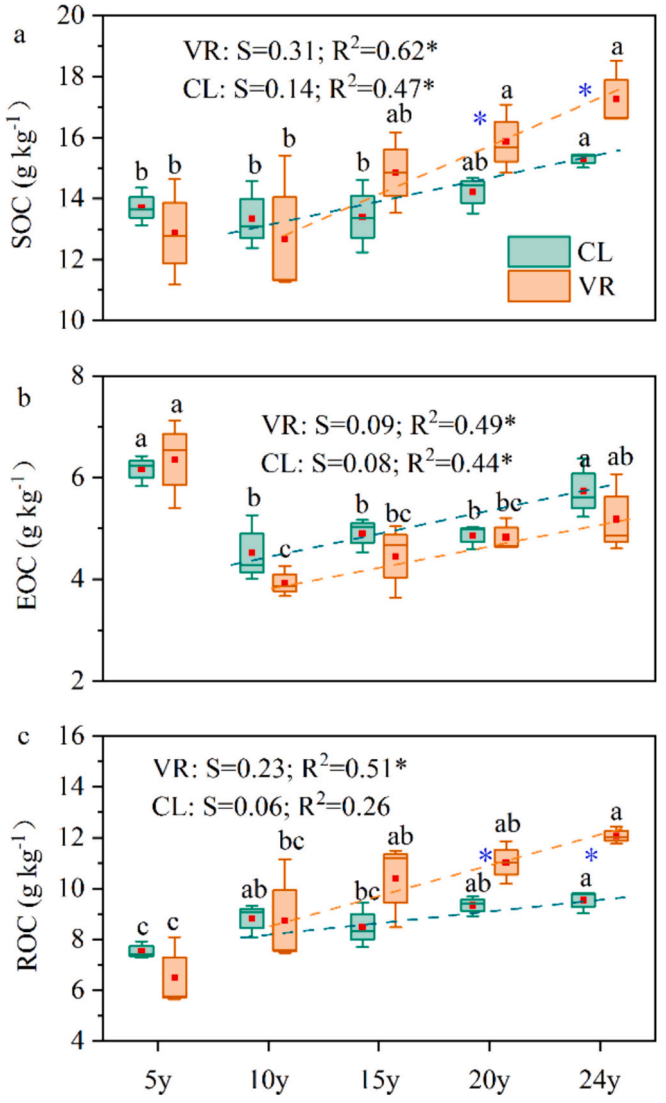

Fig. 1. Variation of soil organic C (SOC; a) and two fractions: easily oxidizable C (EOC; b) and recalcitrant organic C (ROC; c) in natural vegetation restoration (VR, brown) and cropland (CL, green). Brown and green lines indicate linear regressions for the natural vegetation restoration (VR) and cropland (C) soils at Stage II (>10 y after LUCC), respectively. S is the slope of linear regressions, indicating the annual increasing rate of SOC, EOC and ROC. Data are presented as the mean values with standard errors ($N = 3$). Lowercase letters represent significant differences at $P < 0.05$ among the five sampling times with VR or CL soils (one-way ANOVA with LSD test). * represent significant differences at $P < 0.05$ between VR and CL soils (paired-sample *t*-test). The slash dashed lines show the variation tendency for VR (brown) and CL (green) soils.

than did EOC (Fig. S2b).

3.2. Contributions of plant-derived and microbial-derived C to soil organic C

During 24 y of LUCC, there was no noticeable change in amino sugars and MNC until 15 y, and a distinct increase was observed after 20 y of LUCC, both higher in VR than in CL (Fig. 2a–b). The two portions of MNC, FNC and BNC, were also distinctly increased after 20 y of LUCC both in VR and CL; however, only FNC was higher in VR than in CL after 20 y and 24 y of LUCC. The ratio of FNC:MNC decreased after a slight increase, with the transition occurring after 15 y of LUCC (Fig. S3).

In contrast, there was a noticeable increase in lignin phenols and PC in VR and CL each sampled year of LUCC, both of which were higher in VR than in CL across all sample years (Fig. 2c–d). Among the three types of lignin phenols, V-type phenols dominated accounting for 60–87 % of the total, followed by S- and C-type phenols. Additionally, the C/V ratio was lower in VR than in CL across all sampled years (Fig. S4).

Accordingly, the contribution of MNC to SOC was 41 %–84 %, which was not significantly different ($P < 0.05$) between CL and VR, while 14–28 % of SOC derived from plant residues in VR was higher than 3–11 % in CL (Fig. 2e–f). Regression analysis indicated that was SOC positively related to MNC in VR and CL but positively related to PC only in VR. Recalcitrant organic C was positively related to PC in both VR and CL (Fig. 3).

3.3. Effects of biotic and abiotic factors on microbial necromass and plant-derived C

A total of 35 variables were measured and compiled in CL and VR, including abiotic factors of soil geochemical properties (Table S1) and climate conditions (see Fig. S1), bacterial and fungal diversity and community composition (see Table S2). The top three important factors controlling the BNC were TN, AP, and TP in CL, and the relative abundance of Chloroflexi and Firmicutes, TN in VR (Fig. 4a); controlling FNC were AN, TP and the relative abundance of Mucoromycota in CL, and TN, AN and pH in VR (Fig. 4b); controlling PC were TN, MAT, and the relative abundance of Rozellomycota in CL, and TN, the relative abundance of Chloroflexi and Firmicutes in VR (Fig. 4c). Correlation analysis showed that BNC and PC were all significantly ($P < 0.05$) positively related to TN in CL and VR, but related to AP and TP only in CL. MAP was related to BNC and FNC in VR but not in CL. Otherwise, CEC was related to FNC in VR. The relative abundance of Chloroflexi was significantly ($P < 0.05$) positively related to PC and BNC in CL and VR. And the relative abundance of Ascomycota and diversity of fungi were significantly ($P < 0.05$) positively related to PC in CL but not in VR (Fig. 5).

4. Discussion

4.1. Greater increase of soil organic C in natural revegetation than in cropland

The temporal dynamics of SOC supported our hypothesis of a greater increase of SOC in VR compared to CL after 24 y LUCC. Based on the SOC increase rate of 0.31 g kg^{-1} a^{-1} (per year) and soil bulk density of 1.2 Mg m^{-3} in 0.2 m top soil in VR, the carbon sequestration throng of SOC will be 28.27 Gt in the global natural forest with approximately 38 G ha (data from FAO in 2020), which accounts for 8.7 % of global carbon emissions with 322.8 Gt (data from BP Statistical Review of World Energy) in 2020. Although this value is far from encouraging, it can be expected to be persistent. Nevertheless, a switch from natural ecosystems to artificially disturbed ecosystems, such as converting VR to CL, may cause a one-half potential C loss (Fig. 1). In the scenario of converting all the global natural forest to cropland, it is estimated that 15.50 Gt of C will be lost from the topsoil (0–20 cm), equivalent to 4.8 % of global carbon emissions. Therefore, our study emphasized the great potential of using natural revegetation to hedge against carbon emissions and the important implications for global nature-based climate solutions.

In our study, the observed increase in SOC content in VR during Stage II was likely due to the higher inputs of easily decomposable above- and below-ground biomass produced by trees, shrubs, and herbs (Post and Kwon, 2000). The amount of C stored in soil depends on the quantity and quality of organic matter incorporated therein (Hüblová and Frouz, 2021; Paula et al., 2021). Li et al. (2022) found that VR could enhance SOC accumulation through increased plant inputs in terms of plant biomass and C content. Clearly superior to CL, the reduction of external disturbances and the improvement in vegetation coverage after 10 y of VR likely mitigated soil erosion on the sloped study site,

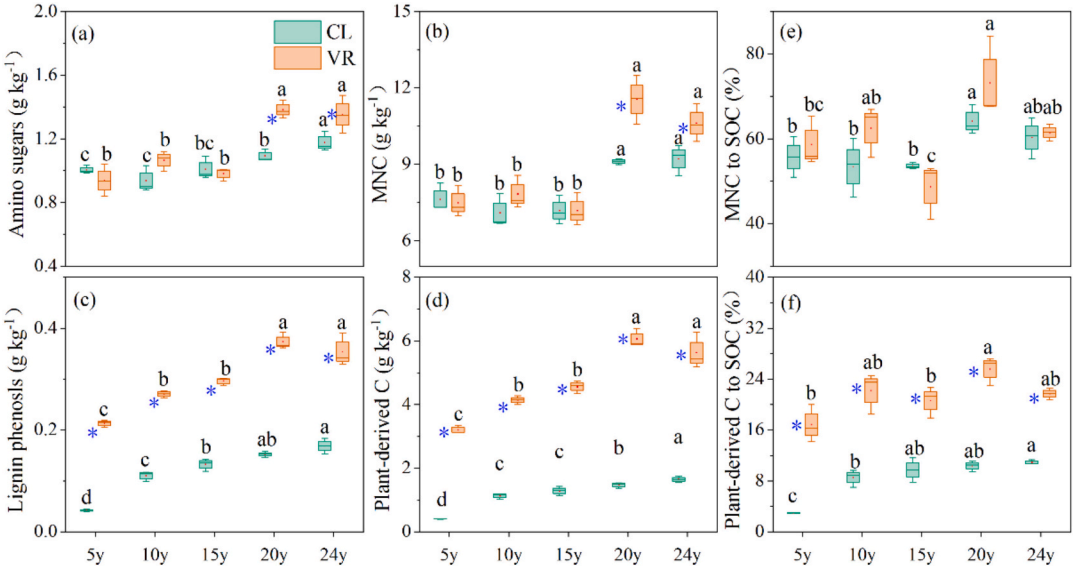

Fig. 2. Contribution of plant- and microbial-derived C to soil organic C (SOC) in natural vegetation restoration (VR; brown) and cropland (CL; green) soils. Contents of amino sugars (a) and microbial necromass (MNC; b), lignin phenols (c) and plant-derived C (d), and the contribution of MNC (e) and plant-derived C (f) to SOC in VR (brown) and CL (green) soils. Lowercase letters represent significant differences at $P < 0.05$ among the five sampling times with VR or CL soils (one-way ANOVA with LSD test). * represent significant differences at $P < 0.05$ between VR and CL soils (paired-sample *t*-test).

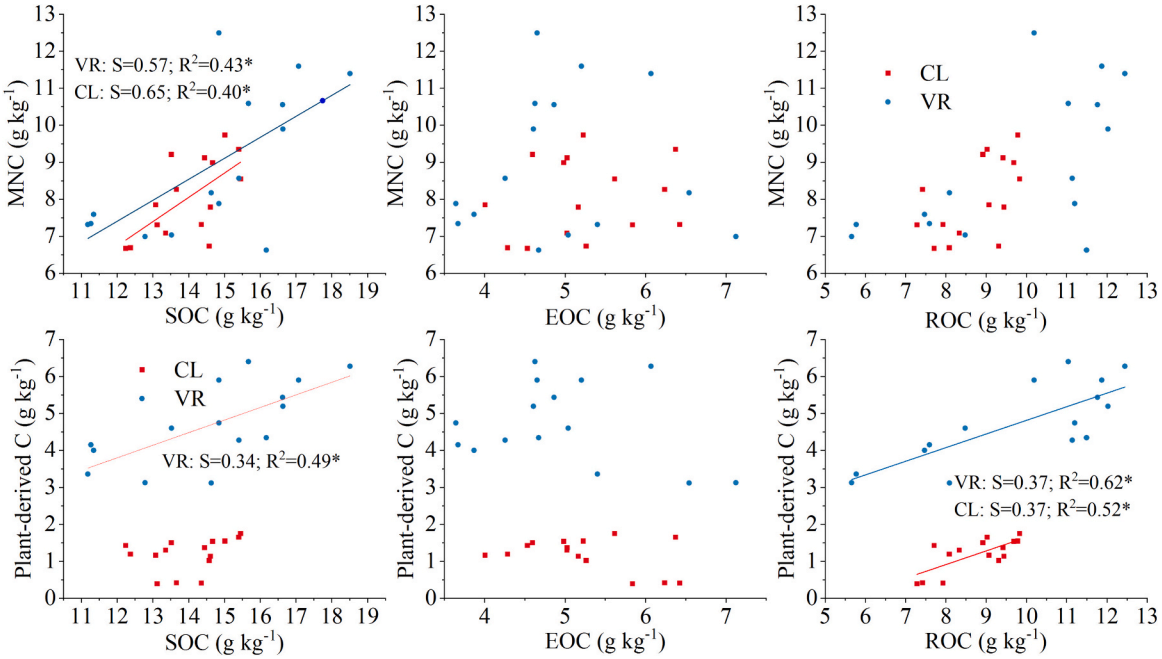

Fig. 3. Regression analysis for plant- and microbial-derived C and soil organic carbon (SOC), easily oxidizable carbon (EOC), and recalcitrant organic carbon (ROC) in natural vegetation restoration (VR, blue) and cropland (CL, red) soils. The solid lines indicate a significant linear relationship ($P < 0.05$). MNC, microbial necromass. S, slope of the solid line. *$P < 0.05$.

contributing to the increase in SOC in VR (Segura et al., 2016; Xiao et al., 2020). Notably, while total SOC showed minimal observable changes, there were evident increases in ROC and decreases in EOC during Stage I of the initial 10 y of LUCC. A higher ROC but lower EOC indicates strong SOC pool stability owing to EOC with short turnover time and susceptibility to oxidative decomposition and mineralization, whereas ROC is considered an important SOC pool stability indicator owing to its long decomposition cycle (Thaysen et al., 2017; Dou et al., 2024). The decrease in EOC content may have been stimulated by unprotected organic matter decomposition and erosion resulting from soil disturbances, as the experiment was set up in freshly ploughed slope land (Wei et al., 2014; Tang et al., 2016). Tillage practices generally disrupt soil aggregates, exposing protected organic matter to microbial decomposition, thereby accelerating labile SOC decomposition (Reda, 2016). Our findings also underscored the significant contribution of ROC to SOC variations, particularly in the VR context. These results were consistent with previous studies on the Loess Plateau, highlighting the key role of ROC in soil carbon sequestration along long-term vegetation successions (Shi et al., 2023). Given that different SOC fractions have different turnover rates and environmental sensitivities, examining the fractions of SOC is important to comprehensively understand SOC stability and long-term formation under future climate change.

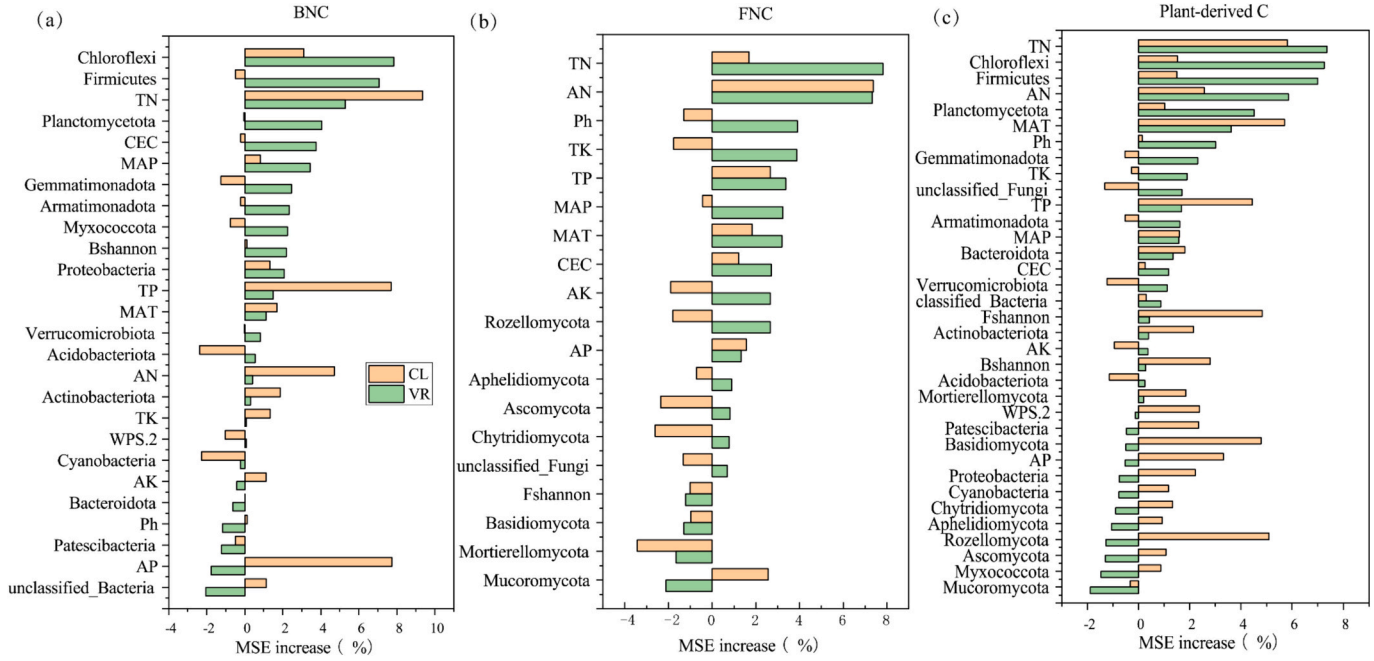

Fig. 4. Relative importance of independent variables for controlling bacterial necromass (a, BNC), fungal necromass (b. FNC), and plant-derived C (c) in natural vegetation restoration (VR; red) and cropland (CL; gray) soils as identified by the percentage increase of the mean squared error (MSE%) using random forests models. AN, alkali-hydrolyzable nitrogen; AP, available phosphorus; AK, available potassium; TN, total nitrogen; TP, total phosphorus; TK, total potassium; CEC, cation exchange capacity. MAT, mean annual temperature; MAP, mean annual precipitation; Bshannon, Shannon index of bacteria; Fshannon, Shannon index of fungi; CAZy-M, the abundance (RPKM: Reads per kilobase per million) of Carbohydrate-Active Enzyme encoding the decomposition of microbial-derived components; CAZy-P, the abundance (RPKM: Reads per kilobase per million) of Carbohydrate-Active Enzyme encoding the decomposition of plant-derived components.

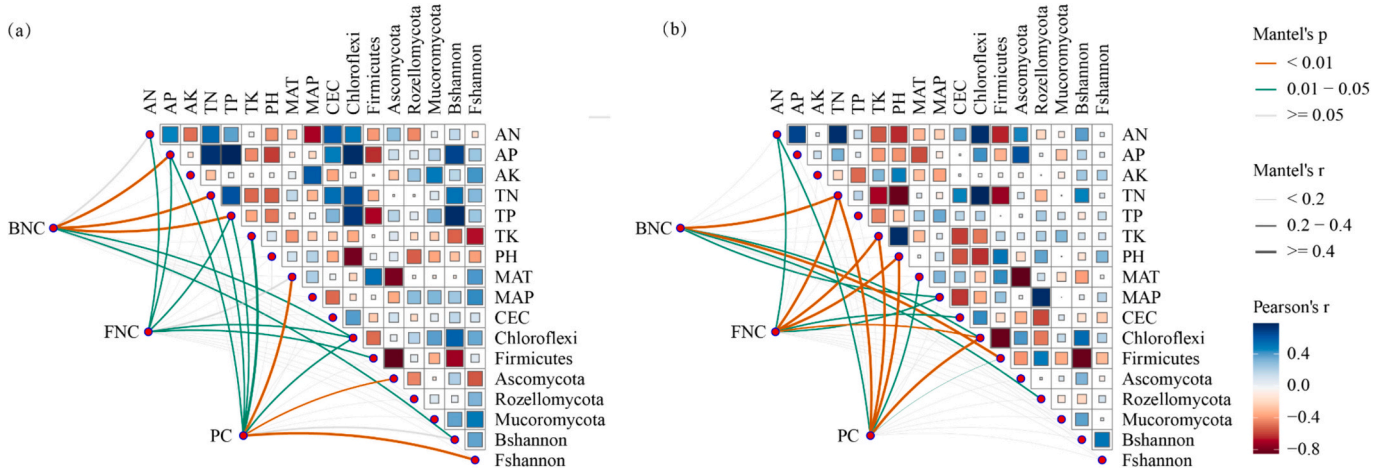

Fig. 5. Partial correlations between bacterial necromass (BNC), fungal necromass (FNC), and plant-derived C (PC) and biotic and abiotic factors in cropland (CL; a) and natural vegetation restoration (VR; b) and soils. The first row shows the factors for which correlations with BNC, FNC, and PC are examined. The color of the square indicates the strength and sign of the correlation. AN, alkali-hydrolyzable nitrogen; AP, available phosphorus; AK, available potassium; TN, total nitrogen; TP, total phosphorus; TK, total potassium; CEC, cation exchange capacity. MAT, mean annual temperature; MAP, mean annual precipitation; Bshannon, Shannon index of bacteria; Fshannon, Shannon index of fungi; Chloroflexi and Firmicutes, the relative abundance of these bacterial phyla; Ascomycota, Rozellomycota and Mucoromycota, the relative abundance of this fungal phylum.

4.2. Increasing contribution of plant-derived but not microbial-derived C to soil organic C in natural revegetation than in cropland

The findings in this study indicated differential contributions of microbial and plant C to SOC formation along the temporal dynamics in VR and CL since LUCC. Although there were greater proportions of microbial-derived C in both CL and VR, there was no difference between them. The higher SOC content in VR was attributed to the higher contribution of PC but not microbial-derived C to SOC. Our analyses revealed that MNC accounted for approximately 50 % of SOC and exhibited insignificant changes over time, which aligned with the findings of Liang et al. (2019), who reported that MNC contributed to 55.6 % of total SOC in temperate agricultural soils based on a global analysis. Microbial necromass is relatively consistent, simple-structured, and characterized by a narrow carbon to nitrogen (C/N) ratio (Cotrufo et al., 2019). Compared to plant residues, microbial-derived C in SOC formation is highly stable because it is less influenced by environmental factors and agricultural management practices (Li et al., 2020). Chen et al. (2021) also observed relatively stable MNC contents in both paddy and upland soils, whereas PC showed wider variations. Furthermore, our

study demonstrated that MNC directly and significantly affected SOC both in VR and CL, highlighting the significant contribution of microbial residues to long-term SOC accumulation compared to plant residues. In contrast, 14–28 % of SOC was derived from plant residues in VR, with approximately three-fold larger stocks of lignin phenols in VR relative to CL (Fig. 2), demonstrating that the enhanced efficiency of SOC sequestration in VR compared to CL was predominantly due to its greater accumulation of PC, as previously observed in forest ecosystems (Zhao et al., 2024) and paddy soils (Chen et al., 2021). With regard to PC, the higher C/V ratios in VR than in CL after 24 y of LUCC (Fig. S4), representing a lower degree of oxidative decomposition (Chen et al., 2021), suggesting that the PC was less decomposed in VR than in CL soils as C decomposition potentials primarily influenced by above-ground plants (Wang et al., 2023). Furthermore, our study demonstrated that PC positively correlated to ROC as well as with SOC in VR (Fig. 3), implying that PC was an important component of stable SOC, contributing to the overall SOC formation in VR. A recent review also indicated that plant-derived compounds could account for >50 % of the stabilized SOC in forest soils (Angst et al., 2021). Compared to MNC, which is more stable but reaches a saturation point, PC, though less protected and more susceptible to decomposition, holds the potential for indefinite accumulation in soil (Cotrufo et al., 2019). Accordingly, SOC might accumulate long-lasting from PC in VR, in-depth emphasizing the effects and importance of long-term carbon sequestration through above-ground plants of natural restoration.

4.3. Divergent controls of plant-derived and microbial-derived C in natural revegetation and cropland

Although the contents of PC and microbial-derived C were influenced by abiotic climate factors and physicochemical properties of the soil in both VR and CL, their primary controls differed. Our study found that soil AP and TP contents affected PC and microbial-derived C in CL but not in VR. Agricultural fields commonly experience intensive management practices, including fertilization, irrigation, and pesticide application. These practices could significantly alter the phosphorus content in the soil, affecting microbial processes and carbon residue accumulation (Li et al., 2023). In contrast, the role of climate factors of MAP in regulating microbial-derived C was significant in VR but not in CL. Natural revegetation experienced less human intervention and exhibited greater ecological complexity, which allowed climate factors to have a more pronounced impact on the regulation of microbial-derived C (Wen et al., 2023). We also found CEC significantly related to FNC in VR, confirming that mineral protection promoted the sequestration of microbial-derived C, as exchangeable cations can serve as cationic bridges between mineral surfaces and functional groups of C (He et al., 2022). Our study highlighted the differences of the effects of environmental factors on the plant and microbial residues in managed and unmanaged ecosystems.

Notably, we observed microorganisms influence PC and microbial-derived C through key species of bacterial and fungal community composition. Specifically, we found that *Chloroflexi* was the dominant bacterial phylum contributing to PC and BNC, and *Ascomycota* was the dominant fungi phylum contributing to PC (Fig. 5). It is possible that while *Chloroflexi* played a role in degrading PC, they also affected the BNC through their own iterative processes (Liang et al., 2017; Liang et al., 2019). *Chloroflexi* have previously been considered soil oligotrophs (Fierer et al., 2007) and are likely specialized in the degradation of plant-derived C. *Ascomycota*, the largest and most diverse fungal phylum, is essential for decomposing organic materials and breaking down recalcitrant compounds with wide substrate utilization (Wang et al., 2021). Our study highlighted the crucial role of the dominant bacterial community in the degradation of plant-derived C and the sequestration of C.

5. Conclusion

In conclusion, based on the temporal dynamics of SOC, plant- and microbial-derived C after 24 y of LUCC, SOC increased more in VR than in CL. The higher SOC content in VR was mainly due to an increased contribution of plant-derived C despite a greater proportion of microbial-derived C in both CL and VR. The dominant abiotic factors controlling plant- and microbial-derived C were soil phosphorus content and climate factor of MAP in CL and VR, respectively. The bacterial phylum of *Chloroflexi* and fungal phylum of *Ascomycota* were the key biotic factors regulating plant- and microbial-derived C through degrading plant residues and formation of microbial necromass. This study elucidates the differential contribution of plant- and microbial-derived organic matter to temporal dynamics of SOC on a field scale. The findings shed light on the underlying mechanisms of long-term SOC sequestration under various land management practices and emphasizes the potential of natural processes to combat global warming.

Supplementary data to this article can be found online at https://doi.org/10.1016/j.scitotenv.2024.174960.

CRediT authorship contribution statement

Hongling Qin: Investigation, Funding acquisition, Formal analysis, Conceptualization. **Yi Liu:** Writing – original draft, Methodology, Investigation, Formal analysis. **Chunlan Chen:** Methodology, Data curation. **Anlei Chen:** Methodology, Formal analysis. **Yuting Liang:** Validation, Investigation. **Carolyn R. Cornell:** Writing – review & editing. **Xue Guo:** Writing – review & editing, Formal analysis. **Edith Bai:** Writing – review & editing, Data curation. **Haijun Hou:** Investigation, Data curation. **Dou Wang:** Methodology, Investigation. **Leyan Zhang:** Software, Investigation. **Jingyuan Wang:** Software, Investigation. **Dongliang Yao:** Software. **Xiaomeng Wei:** Investigation, Formal analysis. **Jizhong Zhou:** Writing – review & editing. **Zhiliang Tan:** Writing – review & editing, Resources. **Baoli Zhu:** Writing – review & editing, Supervision, Investigation, Funding acquisition, Conceptualization.

Declaration of competing interest

The authors declare the following financial interests/personal relationships which may be considered as potential competing interests: Hongling Qin reports financial support was provided by the National Ecosystem Science Data Center. Baoli Zhu reports financial support was provided by the National Key Research and Development Program of China. Baoli Zhu reports financial support was provided by Hunan Science Fund for Distinguished Young Scholars. Hongling Qin reports was provided by the Natural Science Foundation of Hunan. If there are other authors, they declare that they have no known competing financial interests or personal relationships that could have appeared to influence the work reported in this paper.

Data availability

The raw high-throughput sequence data of the bacterial 16S rRNA and fungal ITS genes have been deposited in the GenBank Sequence Read Archive under accession numbers PRJNA1072304 and PRJNA1072313, respectively. The raw metagenomic sequence data reported in this paper were deposited in the Genome Sequence Archive (Genomics, Proteomics & Bioinformatics 2021) in the National Genomics Data Center (Nucleic Acids Res 2022), China National Center for Bioinformation/Beijing Institute of Genomics, Chinese Academy of Sciences (GSA: CRA011114) that are publicly accessible at https://ngdc.cncb.ac.cn/gsa.

Acknowledgements

We thank all members involved in the maintenance of the long-term field experiments, and Dr. Chao Wang of Institute of Applied Ecology CAS and Dr. Xiaowei Guo of Zhejiang University for their insightful discussions. The research was funded by the National Ecosystem Science Data Center (No. NESDC20210204), the National Key Research and Development Program of China (2021YFD1901203; 2021FY100504), Hunan Science Fund for Distinguished Young Scholars (2022JJ10057), and the Natural Science Foundation of Hunan (2022JJ30647; 2022JJ30644).

References

Angst, G., Mueller, K.E., Nierop, K., Simpson, M.J., 2021. Plant-or microbial-derived? A review on the molecular composition of stabilized soil organic matter. Soil Biol. Biochem. 156, 1–3.

Appuhn, A., Joergensen, R.G., 2006. Microbial colonisation of roots as a function of plant species. Soil Biol. Biochem. 38 (5), 1040–1051.

Bastin, J.F., Finegold, Y., Garcia, C., Mollicone, D., Rezende, M., Routh, D., Zohner, C.M., Crowther, T.W., 2019. The global tree restoration potential. Science 365 (6448), 76–79.

Blair, G.J., Lefory, R.D.B., Lisle, L., 1995. Soil carbon fractions based on their degree of oxidation and the development of a carbon management index for agricultural systems. Aust. J. Agr. Res. 46 (7), 1459–1466.

Buckeridge, K.M., Mason, K.E., McNamara, N.P., Ostle, N., Puissant, J., Goodall, T., Griffiths, R.I., Stott, A.W., Whitaker, J., 2020. Environmental and microbial controls on microbial necromass recycling, an important precursor for soil carbon stabilization. Commun. Earth Environ. 1 (1), 36.

Camenzind, T., Mason-Jones, K., Mansour, I., Rillig, M.C., Lehmann, J., 2023. Formation of necromass-derived soil organic carbon determined by microbial death pathways. Nat. Geosci. 16 (2), 115–122.

Chang, R.Y., Liu, S.G., Chen, L.Y., Li, N., Bing, H.J., Wang, T., Chen, X.P., Li, Y., Wang, G. X., 2021. Soil organic carbon becomes newer under warming at a permafrost site on the Tibetan Plateau. Soil Biol. Biochem. 152, 108074.

Chen, G., Ma, S., Tian, D., Xiao, W., Jiang, L., Xing, A., Zou, A., Zhou, L., Shen, H., Zheng, C., Ji, C., 2020. Patterns and determinants of soil microbial residues from tropical to boreal forests. Soil Biol. Biochem. 151, 108059.

Chen, X., Hu, Y., Xia, Y., Zheng, S., Su, Y., 2021. Contrasting pathways of carbon sequestration in paddy and upland soils. Glob. Change Biol. 27, 2478–2490.

Cotrufo, M.F., Ranalli, M.G., Haddix, M.L., Six, J., Lugato, E., 2019. Soil carbon storage informed by particulate and mineral-associated organic matter. Nat. Geosci. 12, 989–994.

Dai, Z.M., Liu, G.F., Chen, H.H., Chen, C.R., Wang, J.K., Ai, S.Y., Wei, D., Li, D.M., Ma, B., Tang, C.X., Brookes, P.C., Xu, J.M., 2020. Long-term nutrient inputs shift soil microbial functional profiles of phosphorus cycling in diverse agroecosystems. ISME J. 14, 757–770.

Dou, W.Q., Xiao, B., Revillini, D., Delgado-Baquerizo, M., 2024. Biocrusts enhance soil organic carbon stability and regulate the fate of new-input carbon in semiarid desert ecosystems. Sci. Total Environ. 918, 170794.

Edwards, J.D., Love, S.J., Phillips, R.P., Fei, S., Domke, G., Parker, J.D., McCormick, M., LaRue, E.A., Schweitzer, J.A., Bailey, J.K., Fordyce, J., Kivlin, S.N., 2024. Long- and short-term soil storage methods other than freezing can be useful for DNA-based microbial community analysis. Soil Biol. Biochem. 191, 109329.

Fierer, N., Bradford, M.A., Jackson, R.B., 2007. Toward an ecological classification of soil bacteria. Ecology 88, 1354–1364.

Friedlingstein, P., 2021. Global carbon budget 2021. Earth Syst. Sci. Data Discuss. 1–191.

Ghani, M.I., Wang, J., Li, P., Pathan, S.I., Sial, T.A., Datta, R., Mokhtar, A., Ali, E.F., Jörg, R., Shaheen, S.M., Liu, M., Abdelrahman, H., 2023. Variations of soil organic carbon fractions in response to conservative vegetation successions on the Loess Plateau of China. Int. Soil Water Conserv. Res. 11 (3), 561–571.

Hautala, K., Peuravuori, J., Pihlaja, K., 1997. Estimation of origin of lignin in humic DOM by CuO oxidation. Chemosphere 35 (4), 0–817.

He, M., Fang, K., Chen, L.Y., Feng, X.H., Qin, S.Q., Kou, D., He, H.B., Liang, C., Yang, Y. H., 2022. Depth-dependent drivers of soil microbial necromass carbon across Tibetan alpine grasslands. Glob. Chang. Biol. 28 (3), 936–949.

Hedges, J.I., Ertel, J.R., 1982. Characterization of lignin by gas capillary chromatography of cupric oxide oxidation products. Anal. Chem. 54 (2), 174–178.

Huang, W., Kuzyakov, Y., Niu, S., Luo, Y., Sun, B., Zhang, J., Liang, Y., 2023. Drivers of microbially and plant-derived carbon in topsoil and subsoil. Glob. Chang. Biol. 29 (22), 6188–6200.

Hüblová, L., Frouz, J., 2021. Contrasting effect of coniferous and broadleaf trees on soil carbon storage during reforestation of forest soils and afforestation of agricultural and post-mining soils. J. Environ. Manage. 290, 112567.

IPCC, 2019. Climate Change and Land: an IPCC special report on climate change, desertification, land degradation, sustainable land management, food security, and greenhouse gas fluxes in terrestrial ecosystems. available at: https://www.ipcc.ch/site/assets/uploads/2019/11/SRCCL-Full-Report-Compiled-191128.pdf (last access: 23 March 2022).

Jung, S.J., Kim, S.H., Chung, I.M., 2015. Comparison of lignin, cellulose, and hemicellulose contents for biofuels utilization among 4 types of lignocellulosic crops. Biomass Bioenergy 83, 322–327.

Kan, Z.R., Liu, W.X., Liu, W.S., Lal, R., Dang, Y.P., Zhao, X., Zhang, H.L., 2022. Mechanisms of soil organic carbon stability and its response to notill: a global synthesis and perspective. Glob. Chang. Biol. 28 (3), 693–710.

Ladau, J., Eloefadrosh, E.A., 2019. Spatial, temporal, and phylogenetic scales of microbial ecology. Trends Microbiol. 27, 662–669.

Langille, M.G., Zaneveld, J., Caporaso, J.G., McDonald, D., Knights, D., Reyes, J.A., Clemente, J.C., Burkepile, D.E., Thurber, R., Knight, R., Beiko, R.G., Huttenhower, C., 2013. Predictive functional profiling of microbial communities using 16S rRNA marker gene sequences. Nat. Biotechnol. 31 (9), 814–821.

Li, J., Zhang, X., Luo, J., Lindsey, S., Zhou, F., Xie, H.T., Li, Y., Zhu, P., Wang, L.C., Shi, Y. L., He, H.B., Zhang, X.D., 2020. Differential accumulation of microbial necromass and plant lignin in synthetic versus organic fertilizer-amended soil. Soil Biol. Biochem. 149, 107967.

Li, Y.Y., Wang, W., Xie, X.L., Yin, C.M., Chen, A.L., 2022. The vegetation succession of ecological recovery process in red soil slope of north Hunan province. Ecol. Environ. Sci. 24, 749–755.

Li, Y., Zhang, W., Li, J., Zhou, F., Liang, X., Zhu, X., He, H., Zhang, X., 2023. Complementation between microbial necromass and plant debris governs the long-term build-up of the soil organic carbon pool in conservation agriculture. Soil Biol. Biochem. 178, 0038–0717.

Liang, C., Schimel, J.P., Jastrow, J.D., 2017. The importance of anabolism in microbial control over soil carbon storage. Nat. microbiol. 2 (8), 1–6.

Liang, C., Amelung, W., Lehmann, J., Kästner, M., 2019. Quantitative assessment of microbial necromass contribution to soil organic matter. Glob. Chang. Biol. 25 (11), 3578–3590.

Lu, R.K., 2000. Agricultural chemical analysis method of soil. Chinese Agric. Sci. Technol. Press 107–108.

Ma, S., Chen, G., Tian, D., Du, E., Xiao, W., Jiang, L., Zhou, Z., Zhu, J., He, H., Zhu, B., Fang, J., 2020a. Effects of seven-year nitrogen and phosphorus additions on soil microbial community structures and residues in a tropical forest in Hainan Island, China. Geoderma 361, 114034.

Ma, T., Dai, G., Zhu, S., Chen, D., Chen, L., Lu, X., Wang, X., Zhu, J., Zhang, Y., He, J., Bai, Y., Han, X., Feng, X., 2020b. Vertical variations in plant-and microbial-derived carbon components in grassland soils. Plant and Soil 446, 441–455.

Ni, H.W., Jing, X.Y., Xiao, X., Zhang, N., Wang, X.Y., Sui, Y.Y., Sun, B., Liang, Y.T., 2021. Microbial metabolism and necromass mediated fertilization effect on soil organic carbon after long-term community incubation in different climates. ISME J. 15, 2561–2573.

Nilsson, R.H., Anslan, S., Bahram, M., Wurzbacher, C., Baldrian, P., Tedersoo, L., 2019. Mycobiome diversity: high-throughput sequencing and identification of fungi. Nat. Rev. Microbiol. 17 (2), 95–109.

Paula, R.R., Calmon, M., Lopes-Assad, M.L., Mendonça, E., 2021. Soil organic carbon storage in forest restoration models and environmental conditions. J. For. Res. 33, 1–12.

Post, W.M., Kwon, K.C., 2000. Soil carbon sequestration and land use change: processes and potential. Glob. Chang. Biol. 6 (3), 317–327.

Qin, H., Yuan, H., Zhang, H., Zhu, Y., Yin, C., Tan, Z., 2013. Ammonia-oxidizing archaea are more important than ammonia-oxidizing bacteria in nitrification and NO_3^--N loss in acidic soil of sloped land. Biol. Fertil. Soils 49 (6), 767–776.

Reda, G.T., 2016. A review on: effect of tillage and crop residue on soil carbon and carbon dioxide emission. J. Environ. Earth Sci. 6, 72–77.

Rennert, T., Georgiadis, A., Ghong, N., Rinklebe, J., 2018. Compositional variety of soil organic matter in mollic floodplain-soil profiles - also an indicator of pedogenesis. Geoderma 311, 15–24.

Schmidt, M.W., Torn, M.S., Abiven, S., Dittmar, T., Guggenberger, G., Janssens, I.A., Kleber, M., Kögel-Knabner, I., Lehmann, J., Manning, D., Nannipieri, P., Rasse, D., Weiner, S., Trumbore, S.E., 2011. Persistence of soil organic matter as an ecosystem property. Nature 478 (7367), 49–56.

Segura, C., Jimenez, M., Nieto, O., Navarro, F.B., Fernandez, O.E., 2016. Changes in soil organic carbon over 20 years after afforestation in semiarid SE Spain. For. Ecol. Manage. 381, 268–278.

Shi, J., Song, M., Yang, L., Zhao, F., Wu, J., Li, J., Yu, Z., Li, A., Shangguan, Z., Deng, L., 2023. Recalcitrant organic carbon plays a key role in soil carbon sequestration along a long-term vegetation succession on the Loess Plateau. Catena 233, 107528.

Tang, Z., Wang, K., Deng, L., Shangguan, Z.P., 2016. Soil organic carbon dynamics following natural vegetation restoration: evidence from stable carbon isotopes (delta C-13). Agric. Ecosyst. Environ. 221, 235–244.

Thaysen, E.M., Reinsch, S., Larsen, K.S., Ambus, P., 2017. Decrease in heathland soil labile organic carbon under future atmospheric and climatic conditions. Biogeochemistry 133, 17–36.

Wang, S., Huang, Y., 2020. Determinants of soil organic carbon sequestration and its contribution to ecosystem carbon sinks of planted forests. Glob. Change Biol. 26, 3163–3173.

Wang, X., Zhang, W., Liu, Y., Jia, Z., Li, H., Yang, Y., Wang, D., He, H., Zhang, X., 2021. Identification of microbial strategies for labile substrate utilization at phylogenetic classification using a microcosm approach. Soil Biol. Biochem. 153.

Wang, S., Chen, D., Liu, Q., Zang, L., Zhang, G., Sui, M., Dai, Y., Zhou, C., Li, Y., Yang, Y., Ding, F., 2023. Dominant influence of plants on soil microbial carbon cycling functions during natural restoration of degraded karst vegetation. J. Environ. Manage. 345, 118889.

Wasige, J.E., Groen, T.A., Rwamukwaya, B.N., Tumwesigye, W., Smaling, E., Jetten, V., 2014. Contemporary land-use/land cover types determine soil organic carbon stocks in south-west Rwanda. Nutr. Cycl. Agroecosyst. 100 (1), 19–33.

Wei, X., Huang, L., Xiang, Y., Shao, M., Zhang, X., Gale, W., 2014. The dynamics of soil OC and N after conversion of forest to cropland. Agric. For. Meteorol. 194, 188–196.

Wen, S.H., Chen, J.Y., Yang, Z.M., Deng, L., Feng, J., Zhang, W., Zeng, X.M., Huang, Q.Y., Baquerizo, M.D., Liu, Y.R., 2023. Climatic seasonality challenges the stability of microbial-driven deep soil carbon accumulation across China. Glob. Chang. Biol. 29 (15), 4430–4439.

Xiao, S., Zhang, J., Duan, J., Liu, H., Wang, C., Tang, C.J., 2020. Soil organic carbon sequestration and active carbon component changes following different vegetation restoration ages on severely eroded red soils in subtropical China. Forests 11 (12), 1304.

Zhang, X., Amelung, W., 1996. Gas chromatographic determination of muramic acid, glucosamine, mannosamine, and galactosamine in soils. Soil Biol. Biochem. 28 (9), 1201–1206.

Zhao, X., Tian, P., Zhang, W., Wang, Q., Guo, P., Wang, Q., 2024. Nitrogen deposition caused higher increases in plant-derived organic carbon than microbial-derived organic carbon in forest soils. Sci. Total Environ. 925, 171752.